

Synthesis, structure, photo- and electroluminescent properties of bis{(4-methyl-N-[2-[(E)-2-pyridyliminomethyl]phenyl)]benzenesulfonamide} zinc(II)

Anatolii S. Burlov^a, Eugenii I. Mal'tsev^b, Valery G. Vlasenko^{c,*}, Dmitrii A. Garnovskii^d, Artem V. Dmitriev^b, Dmitrii A. Lypenko^b, Anatoly V. Vannikov^b, Pavel V. Dorovatovskii^e, Vladimir A. Lazarensko^e, Yan V. Zubavichus^e, Victor N. Khrustalev^f

^a Institute of Physical and Organic Chemistry of Southern Federal University, Stachki Ave. 194/2, Rostov-on-Don 344090, Russian Federation

^b A.N. Frumkin Institute of Physical Chemistry and Electrochemistry of RAS, Leninskii Ave. 31/4, Moscow 119991, Russian Federation

^c Institute of Physics of Southern Federal University, Stachki Ave. 194, Rostov-on-Don 344090, Russian Federation

^d Southern Scientific Centre of Russian Academy of Sciences, Chekhova Ave. 41, Rostov-on-Don 344006, Russian Federation

^e NRC Kurchatov Institute, 1 Acad. Kurchatov Sq., Moscow 123182, Russian Federation

^f Department of Inorganic Chemistry, Peoples' Friendship University of Russia (RUDN University), Miklukho-Maklay Str., 6, Moscow 117198, Russian Federation

ARTICLE INFO

Article history:

Received 17 April 2017

Accepted 23 May 2017

Available online 1 June 2017

Keywords:

Azomethines

Zinc complex

Luminescence

TD-DFT

OLED

ABSTRACT

The synthesis, structure and spectroscopic properties of luminescent Zn(II) complex containing 4-methyl-N-[2-[(E)-pyridinylmethyl]phenyl]benzoesulfimide ligand are described. The Zn(II) complex was characterized by single-crystal X-ray diffraction study. Time-dependent density functional theory calculations at the B3LYP/6-31G* level were performed on Zn(II) complex to interpretation its experimental UV-Vis absorption spectrum. OLED device with Zn(II) complex as light-emitting layer has been fabricated. The electroluminescent spectrum of OLED showed a dominant yellow emission at 525 nm (Commission Internationale de l'éclairage (CIE) coordinates $x = 0.409$ and $y = 0.506$) and a weak shoulder at 650 nm without any other distinguishing emission from host or adjacent layers. The fabricated OLED generated luminance of more than 1000 cd/m² at 16 V, current density 600 mA/cm² and rather low turn-on voltage of ca. 4 V and power efficiency 1 lm/W.

© 2017 Elsevier Ltd. All rights reserved.

1. Introduction

The use of Tang and Van Slyke [1] tris(8-hydroxyquinolino)aluminium Alq₃ for the manufacture of the first OLED devices with green photoluminescence (PL) and quantum yield of about 32%, operating at low voltage (<20 V), gave impetus to the study of metal chelate complexes, and in particular, zinc complexes as electroluminescent layers. The interest in such Zn complexes is due to their high photo- (PL) and electroluminescent (EL) characteristics and electron-transport properties, thermal stability with high glass transition temperature, variability of structures, the relative simplicity of synthesis.

Especially popular are electroluminescent materials that emit in the range of 400–450 nm, blue emitters, as they are not only the main component of red–green–blue full color OLED displays, but the key components in the formation of the white light combination of blue and orange [2].

The PL and EL properties of chelate complexes of zinc containing an azomethine ligand derivatives of 2-hydroxybenzaldehyde (or alkyl)amines have been studied by many authors [3–7]. The fluorescence band maximum of such complexes are observed in $\lambda_{PL} = 480$ –553 nm. On the basis of these compounds as emissive layers has been made a number of electroluminescent devices. For example, the OLED manufactured with the use of zinc complexes, derivatives of salicylic aldehyde with various amines: bis[N-(2-oxybenzoates)cyclohexylamino]zinc, bis[N-(2-oxybenzoates)-4-tert-butylaniline]zinc and N,N'-bis[(oxybenzone)-1,2-phenyldiamine]zinc, emitting in the blue, green and red spectral regions of the spectrum, respectively [5].

The maxima of the bands of EL OLED based on bis[N-(2-oxybenzoates)-4-tert-butylaniline]zinc $\lambda_{EL} = 520$ nm and N,N'-bis[(oxybenzone)-1,2-phenyldiamine]zinc $\lambda_{EL} = 570$ nm underwent a small bathochromic shift compared to the fluorescence of these complexes $\lambda_{PL} = 510$ nm and $\lambda_{PL} = 565$ nm, however, for bis[N-(2-oxybenzoates)cyclohexylamino]zinc, on the contrary, undergoes the largest hypsochromic shift observed from the $\lambda_{PL} = 453$ nm to $\lambda_{EL} = 450$ nm. OLED devices on the basis of these

* Corresponding author.

E-mail address: v.vlasenko@rambler.ru (V.G. Vlasenko).

zinc complexes showed a brightness of 120 cd/m² (8.4 V), 360 cd/m² (12.7 V) and 360 cd/m² (8.5 V) and the current efficiency was 1.4, 15, and 1.7 cd/A, respectively.

The electroluminescent device with an active luminescent layer based on *N,N'*-bis[(2-hydroxybenzylidene)-1,2-phenyldiamine] zinc is made [8]. The device emits in the green spectral region, has the brightness 480 cd/m² at a voltage of 11.8 V and a current density of 26 mA/cm².

Complex of zinc with ligands based on derivatives 8-aminoquinoline used as emitter in the electroluminescent device described in [9], which emits in the blue-green region of the spectrum and has a brightness of 140 cd/m² at a voltage of 19 V and a current density of 1.5 mA/cm², showing an efficiency of 9 cd/A. A manufactured OLED, where the electroluminescent substance used, is one of oxyquinoline zinc complexes of 8-hydroxy-2-methoxyquinoline or 8-hydroxy-2-methylinosine derivatives [10]. This device emits in the green region of the spectrum with the following parameters: brightness of 140 cd/m² is achieved at a voltage of 16 V and a current density of 24 mA/cm², the current efficiency was 4 cd/A. The complex of bis[3-methyl-1-phenyl-4[(quinoline-3-imino)methyl]1-H-pyrazole-5-olato}zinc(II) used as emissive layer in a multilayer electroluminescent device with the structure ITO/CuPc/2TNATA/Spiro-TPD/zinc complex/BCP/BPhen/LiF/Al and emitted in the yellow region of the spectrum ($\lambda_{EL} = 600$ nm) with brightness of 800 cd/m² at a voltage of 10 V, which corresponds to a luminous efficiency of 0.5 Lm/W [11]. Also it was manufactured an electroluminescent device based on the films of bis(2-oxybenzene-4-tret-butylaniline)zinc (99%), and its mixture with the Nile red (1%), emitting in the green and red spectral regions, respectively. The green emission has a brightness of 480 cd/m² at a voltage of 11 V and a current density of 2 mA/cm². The red emission has a luminance of 0.4 cd/m² at a voltage of 11 V and a current density of 30 mA/cm² [12].

The replacing the 2-hydroxy group of the aldehyde fragment in the complexes of zinc azomethine compounds onto the 2-*N*-tosylamine group leads to the change of coordination environment of the zinc ion with of ZnN₂O₂ on with ZnN₄, that in most cases leads to an increase in thermal stability of such complexes and undergoes the largest hypsochromic shift of the bands in the spectra of PL. Such complexes luminesce in the blue region $\lambda_{PL} = 428$ –433 nm with quantum efficiency of PL = 0.23–0.37 [13–21].

In search of new zinc complexes having fluorescence properties and high thermal stability, we have obtained novel azomethine compound 4-methyl-*N*-[2-[(*E*)-pyridinylmethyl]phenyl]benzimidazole (I) and its complex with zinc (II).

2. Experimental

2.1. Materials required and general methods

All starting materials and solvents were used as commercial products. 2-aminopyridine, zinc acetate dihydrate (Alfa Aesar). For the manufacture of electroluminescent devices there were used commercial substances: Phthalocyaninecopper complex (CuPc). ALDRICH. CAS 147-14-8; 4,4',4''-Tris[2-naphthyl(phenyl)amino]triphenylamine (2-TNATA) KINTEC. lot: KZ88BuOMEE0, sales@kintec.hk; TPD –*N,N'*-Bis(3-methylphenyl)-*N,N'*-diphenylbenzidine SIGMA – ALDRICH. CAS 443263-5G; 2,9-Dimethyl-4,7-diphenyl-1,10-phenanthroline (BCP) KINTEC. lot: KZ86BUOHRYO. sales@kintec.hk; 4,7-Diphenyl-1,10-phenanthroline (Bphen) KINTEC. lot: KZ88BuOMEE0. sales@kintec.hk; LiF, ALDRICH. CAS: 7789-24-4. 2-(*N*-Tosylamino)benzaldehyde has been synthesized using the reported procedure [22].

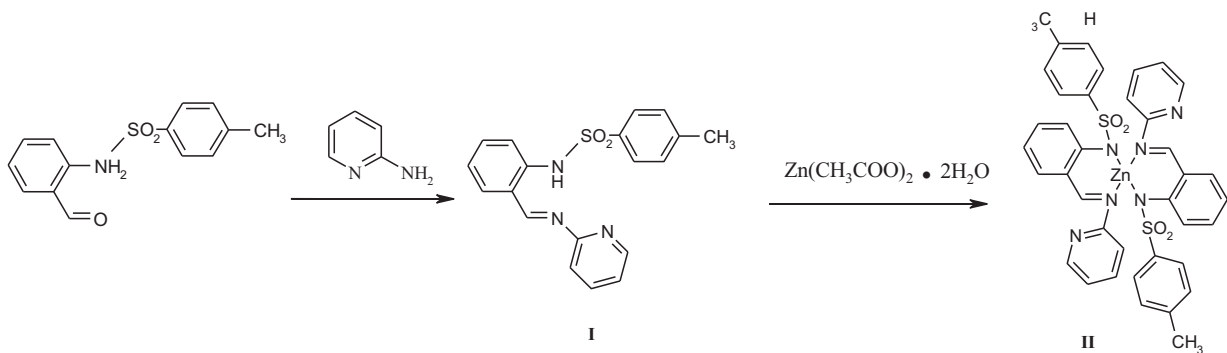
C, H, N, elemental analyses were carried out on a Carlo Erba TCM 480 apparatus using sulfanilamide as the standard. The metal content was determined gravimetrically in the analytical laboratory of the Institute of Physical and Organic Chemistry (SFU, Rostov-on-Don, Russia). Melting points were measured on a Kofler bench.

Infrared spectra (4000–400 cm⁻¹) were recorded on a Varian Excalibur-3100 FT-IR spectrophotometer in KBr pellets.

¹H NMR spectra were measured on a «Varian University-300» spectrometer at ambient temperature in CDCl₃ with the signal of residual 2H of the solvent as the internal reference.

Electron absorption spectra were obtained on a «Varian Cary 100» spectrophotometer, fluorescence spectra were obtained on a «Varian Cary Eclipse» fluorescence spectrophotometer. Spectral grade chloroform from Sigma–Aldrich was used for the preparation of solutions. All UV–Vis and fluorescence spectra were recorded using standard 1 cm quartz cell in CHCl₃ solutions at room temperature at $c = 4.0 \cdot 10^{-5}$ M.

The geometry of complex II in the ground state was fully optimized at the DFT level using GAUSSIAN-03 computer program [23]. For calculations the hybrid three-parameter functional B3LYP [24,25] and the standard split-valence polarization basis set 6-31G(d) [26] were chosen. Simulations of UV–Vis absorption spectra for these molecules were accomplished in the framework of Time Dependent Density Functional Theory (TD-DFT) using optimized atomic structure parameters with account of solvent effects by the standard polarizable continuum model (PCM) with integral equation formalism method [27].



2.2. Ligand synthesis

2.2.1. 4-methyl-N-[2-[(E)-2-pyridyliminomethyl]phenyl]benzenesulfonamide (HL)

A solution containing 0.55 g (2 mmol) of 2-(N-tosylamino)benzaldehyde in 10 ml of toluene was added to the solution of 0.19 g (2 mmol) of 2-aminopyridine in 10 ml of toluene. The mixture was refluxed during 1 h with a Dean-Stark trap until water stripping was completed. The precipitate formed was filtered off and recrystallized from a chloroform-ethanol 1:2 mixture and dried at 150 °C.

Yellow crystals, m.p. = 117–118 °C. Yield 78%. *Anal.* Calc. for $C_{19}H_{17}N_3O_2S$: C, 64.92; H, 4.84; N, 11.96. Found: C, 65.02; H, 4.74; N, 11.84%. IR spectrum in KBr, selected bands, cm^{-1} : 3100–2870 ν (NH), 1621 ν (CH=N), 1342 ν_{as} (SO₂), 1160 ν_s (SO₂). ¹H NMR (CDCl₃), δ (ppm): 2.37 (3H, s, CH₃), 7.09–7.84 (11H, m, C_{Ar}-H), 8.54 (1H, d, ³J = 4.8 Hz, C_{Ar}-H), 9.33 (1H, s, CH=N), 13.13 (1H, s, NH).

2.3. Synthesis of complex

2.3.1. Bis{(4-methyl-N-[2-[(E)-2-pyridyliminomethyl]phenyl]benzenesulfonamide}zinc(II)

A hot solution of 0.35 g (1 mmol) of 4-methyl-N-[2-[(E)-2-pyridyliminomethyl]phenyl]benzenesulfonamide in 25 ml of ethanol was added to solution of 0.11 g (0.5 mmol) zinc acetate dihydrate in 5 ml of ethanol. The reaction mixture was refluxed at 80 °C for 1 h. The precipitate of complex was filtered off and crystallized from a chloroform-ethanol 1:2 mixture and dried at 150 °C.

Yellow crystals, m.p. > 250 °C. Yield 84%. *Anal.* Calc. for $C_{40}H_{34}N_6O_4S_2Cl_6Zn$: C, 47.81; H, 3.41; N, 8.36, Zn, 6.51. Found: C, 47.78; H, 3.59; N, 8.31; Zn, 6.48%. IR spectrum in KBr, selected bands, cm^{-1} : 1611 ν (CH=N), 1272 ν_{as} (SO₂), 1139 ν_s (SO₂). ¹H NMR (CDCl₃), δ (ppm): 2.29 (3H, s, CH₃), 6.87–7.86 (11H, m, C_{Ar}-H), 8.33 (1H, d, ³J = 4.8 Hz, C_{Ar}-H), 9.21 (1H, s, CH=N). UV–Vis spectrum in CHCl₃ (nm): 308, 394. PL spectrum (nm): λ_{PL} = 498.

Table 1
Crystallographic Data for **II-2CHCl₃**.

Compound	II-2CHCl₃
Empirical formula	C ₄₀ H ₃₄ N ₆ O ₄ S ₂ Cl ₆ Zn
<i>f</i> w	1004.94
<i>T</i> (K)	100(2)
Crystal size (mm)	0.20 × 0.20 × 0.02
Crystal system	monoclinic
Space group	C2/c
<i>a</i> (Å)	15.793(3)
<i>b</i> (Å)	16.783(3)
<i>c</i> (Å)	16.237(3)
β (°)	92.08(3)
<i>V</i> (Å ³)	4300.9(14)
<i>Z</i>	4
<i>d_c</i> (g cm ⁻³)	1.552
<i>F</i> (000)	2048
μ (mm ⁻¹)	2.552
$2\theta_{maximum}$ (°)	76.92
Index range	–19 ≤ <i>h</i> ≤ 19 –21 ≤ <i>k</i> ≤ 21 –19 ≤ <i>l</i> ≤ 20
No. of reflections collected	27108
No. of unique reflections	4572 (<i>R</i> _{int} = 0.0851)
No. of reflections with (<i>I</i> > 2σ(<i>I</i>))	3281
Data/restraints/parameters	4572/0/269
<i>R</i> ₁ ; <i>wR</i> ₂ (<i>I</i> > 2σ(<i>I</i>))	0.0760; 0.1057
<i>R</i> ₁ ; <i>wR</i> ₂ (all data)	0.1880; 0.2112
Goodness-of-fit (GOF) on χ^2	1.052
<i>T</i> _{minimum} ; <i>T</i> _{maximum}	0.600; 0.930

2.4. X-ray crystal structure determination

X-ray diffraction data were collected on the ‘Belok’ beamline (λ = 0.96990 Å) of the National Research Center ‘Kurchatov Institute’ (Moscow, Russian Federation) using a Rayonix SX165 CCD detector. A total of 360 images were collected using an oscillation range of 1.0° and φ scan mode, and corrected for absorption using the *Scala* program [28]. The data were indexed, integrated and scaled using the utility *iMOSFLM* in CCP4 program [29]. For details, see Table 1. The structure was determined by direct methods and refined by full-matrix least squares technique on F^2 with anisotropic displacement parameters for non-hydrogen atoms. The hydrogen atoms were placed in calculated positions and refined within riding model with fixed isotropic displacement parameters [$U_{iso}(H)$ = 1.5 $U_{eq}(C)$ for the CH₃-groups and 1.2 $U_{eq}(C)$ for the other groups]. All calculations were carried out using the SHELXTL program [30].

Crystallographic data for **II-2CHCl₃** have been deposited with the Cambridge Crystallographic Data Center, CCDC 1540143. Copies of this information may be obtained free of charge from the Director, CCDC, 12 Union Road, Cambridge CB2 1EZ, UK (Fax: +44 1223 336033; e-mail: deposit@ccdc.cam.ac.uk or www.ccdc.cam.ac.uk).

3. Results and discussion

3.1. Spectroscopic properties

The structure of azomethine HL I has been determined from IR, ¹H NMR and elemental analysis data. The infrared spectrum of the free ligand HL showed a broad band at 2870–3100 cm^{-1} which is assigned to the ν HN-tosyl fragment. The absorption band observed at 1621 cm^{-1} and intense absorption bands at 1342 cm^{-1} and 1160 cm^{-1} are attributed to the ν HC=N and as-/s- vibrations of SO₂-group, respectively.

The ¹H NMR data (in CDCl₃ solution) of the HL showed the resonance signals at 9.33 ppm and 13.13 ppm are attributed to HC=N and NH protons, respectively.

According to the elemental analysis data, the zinc complex **II** possess the general formula ZnL₂·2CHCl₃ (**II-2CHCl₃**). IR spectrum of the complex **II-2CHCl₃** demonstrates disappearance of the band ν NH, whereas the band ν HC=N is reduced by 10 cm^{-1} and observed at 1611 cm^{-1} . The bands at 1272 cm^{-1} (ν_{as} SO₂) and 1139 cm^{-1} (ν_s SO₂) are reduced by 42 cm^{-1} and 21 cm^{-1} compared with HL, respectively.

¹H NMR spectrum of **II-2CHCl₃** displays the disappearance of resonance signal at 13.13 ppm is attributed to NH protons of HL, whereas the resonance signal from HC=N protons is slightly shifted in upfield region compared to the free ligand, indicating that the azomethine nitrogen atom is coordinated to the Zn(II) ion after deprotonation [21,31].

3.2. Molecular and crystal structures of **II-2CHCl₃**

Compound of **II-2CHCl₃** was characterized by single-crystal X-ray diffraction study. Its structure is shown in Fig. 1 along with the atomic numbering scheme and selected bond lengths and angles. The full geometrical parameters for **II-2chcl₃** are available as [Supplementary material](#).

Zinc complex **II-2CHCl₃** possesses overall idealized C₂ (2) symmetry and crystallizes in the monoclinic space group C2/c. The intrinsic C₂ symmetry is remained in the crystal – the molecule occupies a special position on the twofold axis. The zinc atom is a four-coordinated to the two monoanionic *N,N*-bidentate chelating ligands, which are bonded to the metal atom through sulfamide

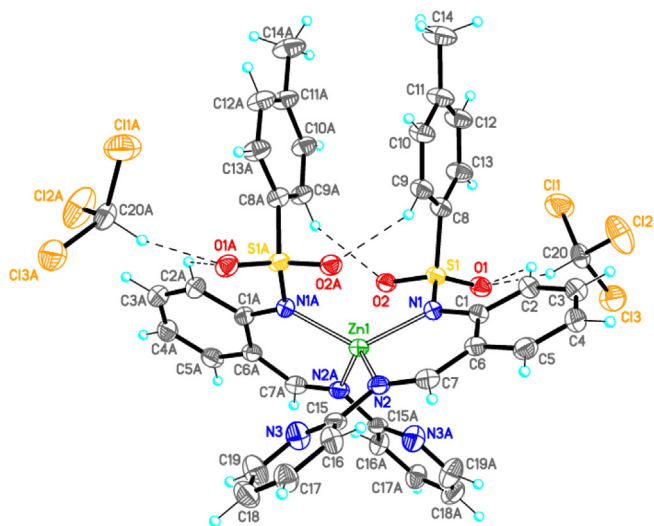


Fig. 1. Molecular structure of **II-2CHCl₃**. Displacement ellipsoids are shown at the 50% probability level. The labeling A denotes symmetrically equivalent atom relative to the twofold axis. Dashed lines indicate the intra- and intermolecular C—H...O hydrogen bonds. Selected bond lengths and angles (Å and): Zn1—N1 2.053(3), Zn1—N2 2.032(3), N1—C1 1.424(5), N2—C7 1.299(5), C1—C6 1.421(5), C6—C7 1.437(5), N1—Zn1—N2 92.39(12), N1—Zn1—N2A 114.12(11), N1—Zn1—N1A 124.54(15), N2—Zn1—N2A 122.12(15), Zn1—N1—C1 126.3(2), Zn1—N2—C7 124.9(2), N1—C1—C6 120.6(3), N2—C7—C6 128.1(3), C1—C6—C7 127.7(4).

and imine nitrogen atoms. The coordination sphere around the zinc atom can be described as distorted tetrahedral (the bond angles range from 92.39(12) to 124.54(15)°, with a dihedral angle between the planar six-membered chelating rings (rms deviation is 0.008 Å) of 81.56(7)°. The smallest N—Zn—N angles are the intrachelate, and the largest one is the *N*_{sulfamide}—Zn—*N*_{sulfamide}. The weak intramolecular Zn1...O2/Zn1...O2A and Zn1...N3/Zn1...N3A interactions at the distances of 2.812(2) and 2.906(4) Å, respectively, might contribute to the distortion of the zinc coordination polyhedron. Taking into account these interactions, the coordination polyhedron of the Zn atom could be described as a bicapped tetrahedron. The molecular geometry observed for complex **II-2CHCl₃** is supported by the four intramolecular C2—H2...O1/C2A—H2A...O1A [C...O 3.012(5), H...O 2.38 Å, ∠C—H...O 124°] and C9—H9...O2A/C9A—H9A...O2 [C...O 3.306(4), H...O 2.44 Å, ∠C—H...O 152°] hydrogen bonds. The Zn—N bond distances (2.032(3) and 2.053(3) Å) are slightly longer than those found in the other related homoleptic zinc complexes with *N,N*-bidentate ligands [32–36]. Apparently, this fact may be also explained by the additional weak intramolecular Zn...O and Zn...N interactions.

In the crystal, complex **II-2CHCl₃** forms the strong enough H-bonded adduct with two solvate chloroform molecules by the two intermolecular C20—H20...O1/C20A—H20A...O1A hydrogen bonds [C...O 3.130(5), H...O 2.17 Å, ∠C—H...O 159°] (Fig. 1). Further the H-bonded adducts are linked by the intermolecular secondary Cl2...Cl2 [−*x*, *y*, ½−*z*] interactions (3.173(3) Å) into zigzag-like chains propagating toward [100] (Fig. 2).

3.3. Electronic absorption spectra and photoluminescence

Electronic absorption spectra and photoluminescence of the complex **II-2CHCl₃** were investigated. To interpret the experimental bands of the electronic absorption spectrum of complex **II-2CHCl₃** there were carried out quantum-chemical calculations in the approximation TD-DFT taking into account the solvent of chloroform.

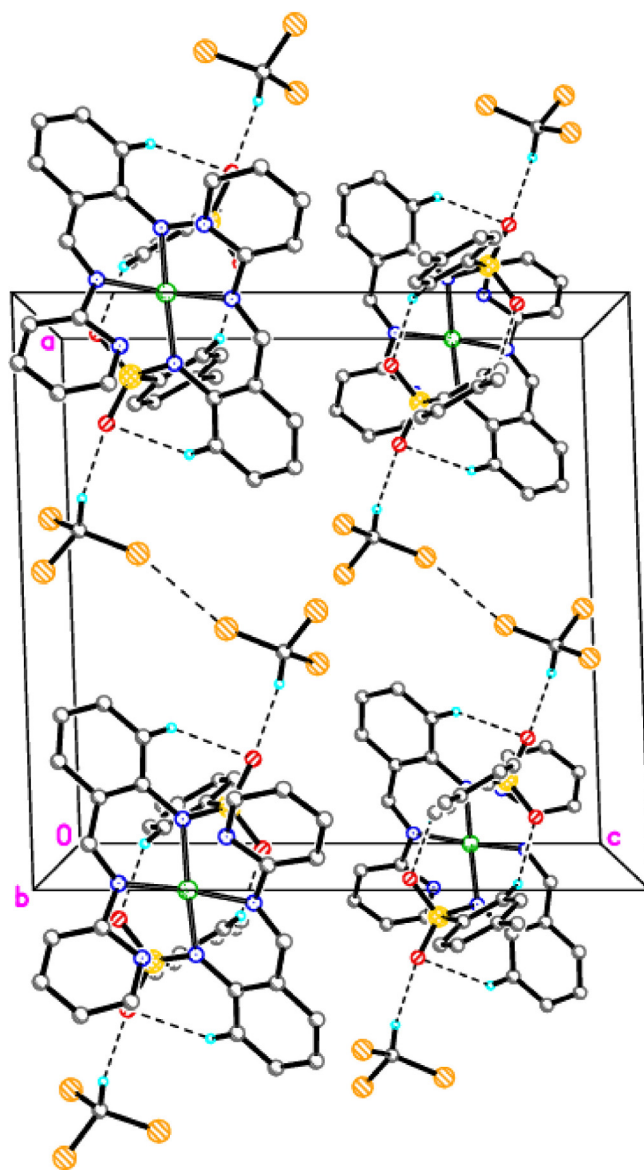


Fig. 2. Crystal structure of **II-2CHCl₃** demonstrating the zigzag-like chains propagating toward [100]. Only hydrogen atoms participating in the formation of hydrogen bonds are shown. Dashed lines indicate the intra- and intermolecular C—H...O hydrogen bonds and intermolecular secondary Cl...Cl interactions.

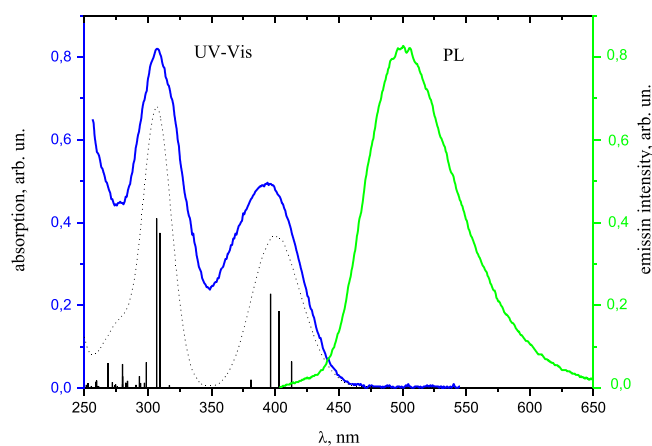


Fig. 3. Experimental electronic spectra (full blue line) registered at 298 K in CH₂Cl₂ and simulated electronic spectra (dashed black line) calculated by TD-DFT and Photoluminescence spectrum (full green line) for complex **II-2CHCl₃**. (Color online.)

The Fig. 3 shows the experimental electronic absorption spectrum of **II-2CHCl₃** in comparison with the results of TD-DFT calculations. In Fig. 3 also presents the photoluminescence spectrum of compound **II-2CHCl₃**. Upon excitation **II-2CHCl₃** the photoluminescence spectrum has a maximum at $\lambda_{\text{PL}} = 498$ nm and undergoes bathochromic shift relative to HL (104 nm). The theoretical electronic excitation energy, wavelengths and oscillator strengths of electronic transitions are listed in Table 2. This Table 2 also presents the interpretation of the specific ways the main electronic transitions, indicating their contributions to the formation of absorption bands.

The electronic absorption spectrum of **II-2CHCl₃** in chloroform shows two main absorption bands at $\lambda_{\text{abs}} = 308$ nm and $\lambda_{\text{abs}} = 394$ nm. Comparison of experimental and calculated absorption spectra of complex **II** shows their good agreement to within a few nm.

The transition metal complexes usually show three types of electronic excitation bands: d–d transitions; transitions metal-to-ligand charge transfer (MLCT) and ligand-to-metal charge transfer (LMCT); transitions intraligand charge-transfer (ILCT) and

negligently transitions charge-transfer (LLCT). The absorption band at 394 nm in the experimental UV–Vis spectrum of complex **II-2CHCl₃** correspond to the three main theoretical electronic transitions (at 412.88, 402.80 and 396.33 nm) with high oscillator strengths. All three crossings are determined by the transitions between the frontier orbitals HOMO → LUMO, HOMO–1 → LUMO, HOMO → LUMO + 1, respectively, with the maximum contributions from 87 to 96%. In Fig. 4 shows the isosurfaces of frontier MO and the relevant electronic transitions for complex **II**. Analysis of the MO shapes shows that for π (HOMO) and π^* (LUMO) the electron density localized in on azomethine aminopyridine ligand. As can be seen from Fig. 3 for the long-wavelength transition is the main type as LLCT charge transfer between different aminopyridine ligands of the complex $\pi \rightarrow \pi^*$, whereas the other two correspond to the transition type ILCT charge-transfer within the same aminopyridine ligand.

For the second intense absorption bands of the experimental spectrum of complex **II-2CHCl₃** at $\lambda_{\text{abs}} = 308$ nm can be assigned to two electronic transition HOMO–3 → LUMO and

Table 2

Calculated wavelengths λ , the energy of vertical electronic transitions E between the relevant frontier MO, contributions from different electronic transitions and oscillator strengths f for **II** obtained from TD-DFT calculations.

λ , nm	E (eV)	Electronic transitions, (weight ^a , %)	f	Assignment
412.88	3.00	HOMO → LUMO (96)	0.06	LLCT
402.80	3.08	HOMO–1 → LUMO (90)	0.18	ILCT
396.33	3.13	HOMO → LUMO + 1 (87)	0.23	ILCT
309.35	4.01	HOMO–3 → LUMO (71)	0.37	ILCT
		HOMO–2 → LUMO + 1 (8)		
306.86	4.04	HOMO–3 → LUMO (6)	0.41	LLCT
		HOMO–2 → LUMO + 1 (73)		
298.67	4.15	HOMO–4 → LUMO (89)	0.06	LLCT

^a Only the main transitions are reported.

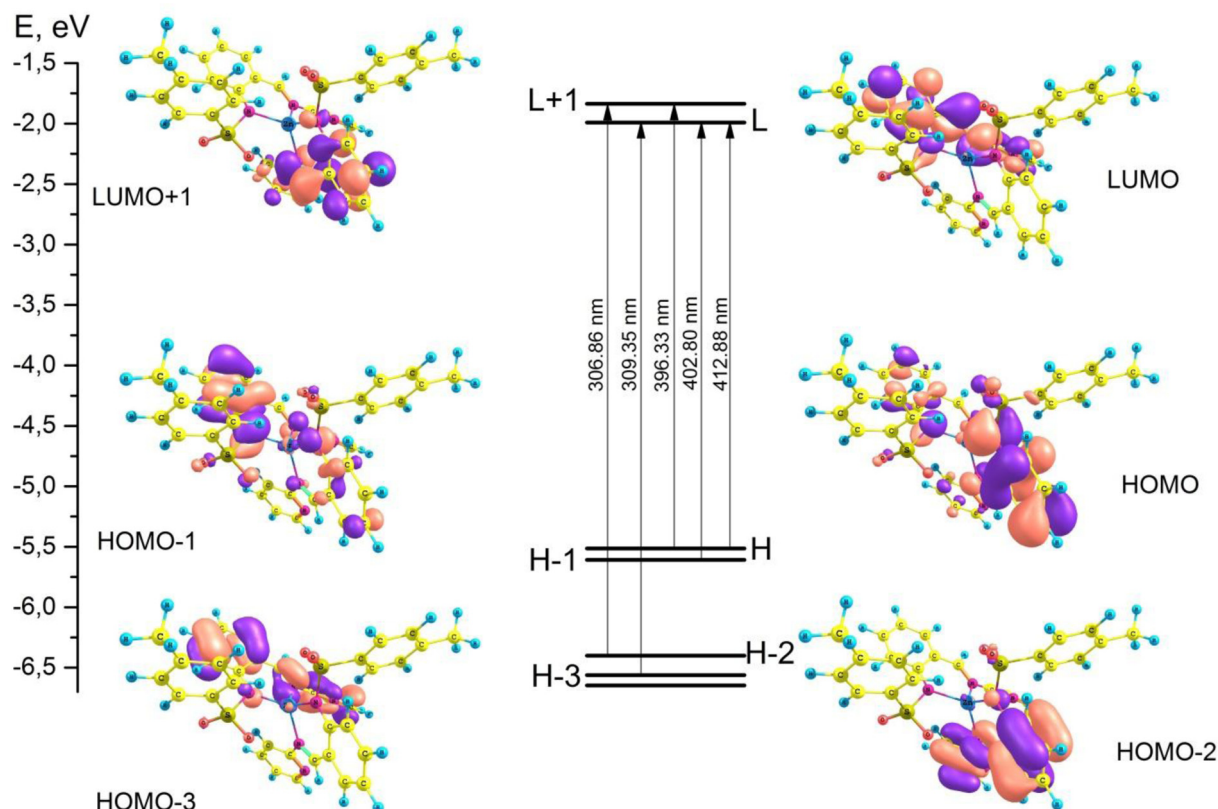


Fig. 4. Frontier molecular orbitals and associated electronic transitions for zinc complex **II**.

HOMO–2 → LUMO + 1 with very close energies and high oscillator strength (around 0.4). These electronic transitions are also responsible $\pi \rightarrow \pi^*$ transfers charge aminopyridine azomethine ligands and belong to two different types of ILCT and LLCT transitions, respectively. Any d-d or MLCT transitions were not found in our calculations, as the ion Zn(II) has a completely filled d-shell. This result is confirmed by the absence of any absorption bands in the wavelength region of the experimental electronic spectra of Zn (II) set.

3.4. Electroluminescent properties of the complex **II-2CHCl₃**

In order to study the electroluminescent properties of the complex **II-2CHCl₃** as phosphor, a multilayered OLED structure was fabricated. It consisted of a pre-cleaned ITO glass substrate coated oxide (15 ohm/sq) as the anode, copper phthalocyanine (CuPc) hole-injecting layer (5 nm), 4,4',4''-Tris[2-naphthyl(phenyl)amino]triphenylamine (2-TNATA) hole-transporting layer (35 nm), *N,N'*-Bis(3-methylphenyl)-*N,N'*-diphenylbenzidine (TPD) electron-blocking layer (6.5 nm), light-emitting layer – complex **II-2CHCl₃** (23 nm), 2,9-dimethyl-4,7-diphenyl-1,10-phenanthroline (BCP) hole-blocking layer (5 nm), 4,7-diphenyl-1,10-phenanthroline (Bphen) electron-transporting layer (26 nm), LiF electron-injecting layer (0.8 nm) and aluminum cathode (100 nm). In the manufacture of the OLED only thermal vacuum deposition technique was used. The complex **II-2CHCl₃** demonstrated high thermal stability. The light-emitting area was 0.3 cm². Electrical and light-emitting properties were measured in an argon environment. Luminance Commission Internationale de l'éclairage (CIE) color coordinates (Fig. 5, insert), current–voltage and brightness–voltage curves of electroluminescent device (Fig. 6) were measured using computer controlled spectrophotometer Ava Spec 2048, Sours Meter Keithley 2601, Keithley 6485 and photometer TKA-04/3.

The EL spectrum showed a dominant yellow emission at 525 nm and a weak shoulder at 650 nm without any other distinguishing emission from host or adjacent layers, indicating effective energy transfer from the host molecules to the dopant. CIE coordinates of the emission band were $x = 0.409$ and $y = 0.506$. Device efficiency was determined by measuring the light output only in

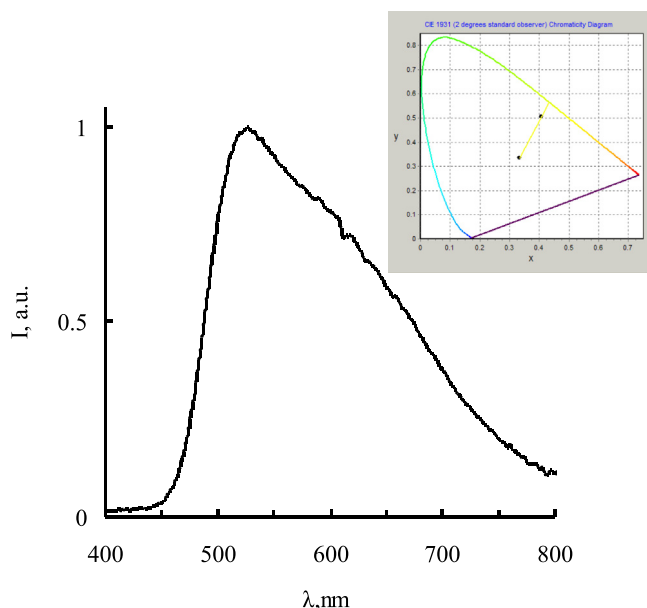


Fig. 5. Electroluminescence spectrum for the complex **II-2CHCl₃** and its CIE color coordinates.

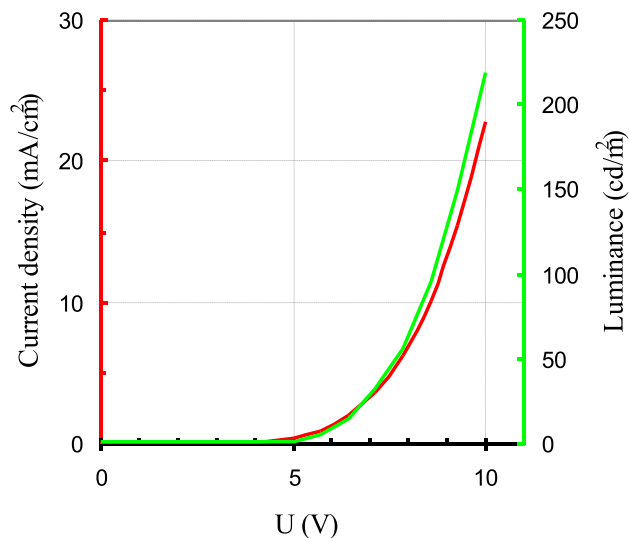


Fig. 6. Current density and luminance as a function of operating voltage for the electroluminescent device.

the front direction. The fabricated OLED generated luminance of more than 1000 cd/m² at 16 V, current density 600 mA/cm² and rather low turn-on voltage of ca. 4 V and power efficiency 1 lm/W.

4. Conclusion

The azomethine compound 4-methyl-N-[2-[(E)-pyridinylmethyl]phenyl]benzothioamide and its zinc complex were synthesized and fully characterized by IR, ¹H NMR, UV–Vis spectroscopy, and elemental analysis. Bands in experimental UV–Vis spectrum have been assigned based on computational results. Photo- and electroluminescent properties of zinc complex have been investigated. The performance of a new phosphorescent complex as an emitter in OLED multilayered structure had been investigated. A device exhibiting stable yellow electrophosphorescence has been fabricated. These preliminary results indicated that zinc complex may be looked upon as a promising light-emitting material for the development of yellow OLED light sources.

Acknowledgements

This work was supported financially by the Ministry of Education and Science of the Russian Federation (Project 4.5388.2017/8.9).

The XRD analysis was supported by the Ministry of Education and Science of the Russian Federation (the Agreement number 02.a03.21.0008).

Appendix A. Supplementary data

CCDC 1540143 contains the supplementary crystallographic data for **II**. These data can be obtained free of charge via <http://dx.doi.org/10.1016/j.poly.2017.05.045>, or from the Cambridge Crystallographic Data Centre, 12 Union Road, Cambridge CB2 1EZ, UK; fax: (+44) 1223-336-033; or e-mail: deposit@ccdc.cam.ac.uk. Supplementary data associated with this article can be found, in the online version, at <http://dx.doi.org/10.1016/j.poly.2017.05.045>.

References

- [1] C.W. Tang, S.A. VanSlyke, *Appl. Phys. Lett.* 51 (1987) 913.
- [2] A.P. Pushkarev, M.N. Bochkarev, *Russ. Chem. Rev.* 85 (2016) 1338.

- [3] L. Chen, J. Qiao, J. Xie, L. Duan, D. Zhang, L. Wang, Y. Qiu, L. Chen, *Inorg. Chim. Acta* 362 (2009) 2327.
- [4] A.P. Pivovarov, M.G. Kaplunov, I.K. Yakushchenko, M.Yu. Belov, G.V. Nikolaeva, O.N. Efimov, *Russ. Chem. Bull. (Int. Ed.)* 51 (2002) 67.
- [5] M.G. Kaplunov, I.K. Yakushchenko, S.S. Krasnikova, S.N. Shamaev, A.P. Pivovarov, O.N. Efimov, *Russ. Chem. Bull. (Int. Ed.)* 53 (2004) 2148.
- [6] J. Xie, J. Qiao, L. Wang, J. Xie, Y. Qiu, *Inorg. Chim. Acta* 358 (2005) 4451.
- [7] Y. Hamada, T. Sano, M. Fujita, T. Fujii, Y. Nishio, K. Shibata, *Jpn. J. Appl. Phys.* 32 (1993) 511.
- [8] M.G. Kaplunov, S.S. Krasnikova, I.K. Yakushchenko, S.N. Shamaev, A.P. Pivovarov, O.N. Efimov, O.N. Ermakov, S.A. Stakharny, *Mol. Cryst. Liq. Cryst.* 426 (2005) 287.
- [9] S.S. Krasnikova, I.K. Yakushchenko, S.N. Shamaev, M.G. Kaplunov, *Mol. Cryst. Liq. Cryst.* 468 (2007) 87.
- [10] M.G. Kaplunov, I.K. Yakushchenko, S.S. Krasnikova, A.P. Pivovarov, I.O. Balashova, *High Energ. Chem.* 42 (2008) 563.
- [11] A.S. Burlov, V.G. Vlasenko, A.V. Dmitriev, V.V. Chesnokov, A.I. Uraev, D.A. Garnovskii, Y.V. Zubavichus, A.L. Trigub, I.S. Vasilchenko, D.A. Lypenko, E.I. Mal'tsev, T.V. Lifintseva, G.S. Borodkin, *Synth. Met.* 203 (2015) 156.
- [12] A.P. Pivovarov, M.G. Kaplunov, O.N. Efimov, I.K. Yakushchenko, M.Y. Belov, *Mol. Cryst. Liq. Cryst. Sci. Tech., Sect. A. Mol. Cryst. Liq. Cryst.* 361 (2001) 263.
- [13] A.V. Metelitsa, A.S. Burlov, S.O. Bezuglyi, A.D. Garnovskii, V.A. Bren, V.I. Minkin, N.N. Kharabaev, RF Patent No. 2295527 (2007).
- [14] A.V. Metelitsa, A.S. Burlov, S.O. Bezuglyi, I.G. Borodkina, I.S. Vasilchenko, A.D. Garnovskii, S.A. Mashchenko, G.S. Borodkin, D.A. Garnovskii, V.I. Minkin, RF Patent No. 2395512 (2010).
- [15] M.R. Bormejo, M. Vazques, J. Sanmartín, A.M. García-Deibe, M. Fondo, C. Lodeiro, *New J. Chem.* 26 (2002) 1365.
- [16] A.V. Metelitsa, A.S. Burlov, S.O. Bezuglyi, I.G. Borodkina, V.A. Bren, A.D. Garnovskii, V.I. Minkin, *Russ. J. Coord. Chem.* 32 (2006) 858.
- [17] A.S. Burlov, D.A. Garnovskii, L.I. Kuznetsova, N.V. Volbushko, O.Yu. Korshunov, O.T. Asmaev, B.I. Kharisov, L.M. Blanco, A.D. Garnovskii, *Russ. J. Coord. Chem.* 24 (1998) 857.
- [18] A.D. Garnovskii, A.S. Burlov, A.V. Metelitsa, I.G. Borodkina, K.A. Lysenko, S.O. Bezuglyi, E.D. Garnovskaya, E.V. Sennikova, G.S. Borodkin, D.A. Garnovskii, *Russ. J. Gen. Chem.* 80 (2010) 292.
- [19] A.S. Burlov, E.I. Mal'tsev, V.G. Vlasenko, A.V. Dmitriev, D.A. Lypenko, D.A. Garnovskii, A.I. Uraev, G.S. Borodkin, A.V. Metelitsa, *Russ. Chem. Bull.* 63 (2014) 1759.
- [20] A.S. Burlov, V.V. Chesnokov, V.G. Vlasenko, D.A. Garnovskii, E.I. Mal'tsev, A.V. Dmitriev, D.A. Lypenko, G.S. Borodkin, Y.V. Revinskii, *Russ. Chem. Bull.* 63 (2014) 1753.
- [21] N.I. Chernova, Y.S. Ryabokobylko, V.G. Brudz, B.M. Bolotin, *Zh. Org. Khim.* 7 (1971) 1680.
- [22] M.J. Frisch, G.W. Trucks, H.B. Schlegel, et al., *Gaussian 03, Revision A.1*, Gaussian Inc, Pittsburgh PA, 2003.
- [23] C. Lee, W. Yang, R.G. Parr, *Phys. Rev.* 37 (1988) 785.
- [24] A.D. Becke, *J. Chem. Phys.* 98 (1993) 5648.
- [25] G.A. Petersson, A. Bennett, T.G. Tensfeldt, M.A. Allaham, W.A. Shirley, J. Mantzaris, *J. Chem. Phys.* 89 (1988) 2193.
- [26] J. Tomasi, B. Mennucci, R. Cammi, *Chem. Rev.* 105 (2005) 2999.
- [27] P.R. Evans, *Acta Cryst. D* 62 (2005) 72.
- [28] T.G. Battye, L.O. Kontogiannis, H.R. Johnson, Powell, A.G.W. Leslie, *Acta Cryst. D* 67 (2011) 271.
- [29] G.M. Sheldrick, *Acta Cryst. C* 71 (2015) 3.
- [30] A.S. Burlov, V.G. Vlasenko, N.I. Makarova, K.A. Lyssenko, V.V. Chesnokov, G.S. Borodkin, I.S. Vasilchenko, A.I. Uraev, D.A. Garnovskii, A.V. Metelitsa, E.I. Mukhanov, T.V. Lifintseva, I.V. Pankov, *Polyhedron* 107 (2016) 153.
- [31] J. Castro, S. Cabaleiro, P. Pérez-Lourido, J. Romero, J.A. García-Vázquez, A. Sousa, *Z. Anorg. Allg. Chem.* 628 (2002) 1210.
- [32] D. Martin, M. Rouffet, S.M. Cohen, *Inorg. Chem.* 49 (2010) 10226.
- [33] K. Pang, Y. Rong, G. Parkin, *Polyhedron* 29 (2010) 1881.
- [34] C.-H. Wang, C.-Y. Li, C.-H. Lin, Y.-C. Liu, B.-T. Ko, *Inorg. Chem. Comm.* 14 (2011) 1456.
- [35] C.-H. Wang, C.-Y. Li, B.-H. Huang, C.-C. Lin, B.-T. Ko, *Dalton Trans.* 42 (2013) 10875.